Laser and Particle Beams (1984), *vol.* 2, *part* 2, *pp.* 129–140
Printed in Northern Ireland

A fundamental theory of high power thyratrons for high power laser and beam applications III: the production of radiation

By J. A. KUNC, D. E. SHEMANSKY, AND M. A. GUNDERSEN
University of Southern California, Los Angeles, CA 90089-0484

(Received 12 September 1983)

The radiation characteristics of a high-current hydrogen thyratron plasma have been modeled in order to study this aspect of the physics of the conductive phase of thyratron operation. The intensities and radiative energy efficiencies of the atomic and molecular systems have been calculated in detail. A model is developed that is useful for studies of photoemission. For discharge parameters $T_e \approx 1$ eV, ionization fraction of $\sim 10^{-2}$ and background density of 10^{16} cm^{-3}, the total power of the emitted radiation is estimated to be of the order of 5% of the total input power during the conductive phase.

1. Introduction

This paper considers quantitatively the production and spectral content of radiation produced by the plasma in a hydrogen glow-discharge. This discharge, described below, is characteristic of a hydrogen thyratron. The production of radiation in a plasma, the detailed spectral content of the radiation, and the specific excitation processes, are important in the operation of various gas-phase devices, including switches such as thyratrons, flashlamps, and incoherent optical pumping sources. The quantitative understanding of such devices is at present very limited. For example, the relative intensity of spectral lines can provide diagnostic information about the electron energy distribution function, (which in turn allows determination of transport parameters such as conductivity), provided a detailed understanding of specific collisional and radiative processes exists for the plasma under consideration. Furthermore, the operation of these devices is often critically dependent on the relative role of specific excitation processes. However, because these plasmas are complex, and the analysis of radiative and collisional processes requires consideration in detail of many processes, at the present time there is a somewhat limited, and only qualitative, understanding of most devices.

This work considers the production of radiation in the plasma that exists during the conductive (closed) phase in a high-current hydrogen discharge, and is a continuation of a series of papers on the physics of high-current thyratrons (Kunc & Gundersen 1982; Kunc *et al.* 1983; Kunc & Gundersen 1983a; Kunc & Gundersen 1983b). A hydrogen thyratron, ordinarily considered a low pressure switch, has typically a hydrogen pressure of the order of 0·5 Torr. In a typical device, the current density may be of the order of 10 to 60 A/cm^2 and the electron distribution function is Maxwellian, with an electron temperature of ~ 1 eV and an electron density $\sim 10^{14}$ cm^{-3} (Kunc & Gundersen 1982; Kunc & Gundersen 1983a). This plasma is important for device applications, but is also of more general interest, because the degree of ionization is unusually high. The electron density is of the order of 1% of the neutral density and, because of

0263-0346/84/0002-0129$05.00

this, the plasma properties are not a simple function of the neutral density—(e.g., of E/N, where E is the electric field and N is the background neutral density). The discharge cannot be properly characterized without taking into account the substantial effect of a low electron temperature, large electron density, and concomitant high electron-electron collision rate (Kunc and Gundersen, 1983b).

The radiation incident on the walls and electrodes of the device will produce charged particles and thus will affect the conductivity and maintenance of the plasma. It is of particular interest to consider the production of charged particles at the cathode of many devices, in order to consider the effect on the electron emission properties of the cathode, and the effect on the cathode potential fall. In order to consider these problems, it is necessary to analyze the processes responsible for the production of radiation. The model that is presented here should be suitable for the analysis of photoemissive properties of many materials that can be in contact with a plasma of this type.

It is assumed for this analysis that the most important processes for excitation of atomic and molecular states are the interactions of atoms and molecules with (i) radiation, and (ii) electrons. Heavy particle interactions are neglected as sources of electronic excitation because of the dominance of electron collisions (Kunc *et al.* 1983; Kunc & Gundersen 1983a).

Heavy particle-wall collisions are also neglected as a source of electronic excitation. Although the efficiencies of these processes are not well understood, calculations indicate that they are low in discharges with conditions similar to those present in this plasma (Hiskes *et al.* 1982; Hiskes 1982). Detailed discussions of the assumptions made in the present work can be found in papers of Kunc *et al.* (1983) and Kunc & Gundersen (1983a).

In estimating the radiation intensity, transitions are primarily considered which are strong in the visible and ultraviolet. This is because these photons are mainly responsible for the production of energy that is radiated out of the plasma volume. Furthermore, these lines are sufficiently energetic to interact with a wall or electrode and produce electrons through photoemission.

2. Molecular excitation and radiative processes

The major source of molecular excitation is assumed to be electron collisions, as indicated above. Model calculations are based on the work of Shemansky & Ajello (1983), using cross-sections given by Ajello *et al.* (1983). Most of the energy in radiation produced from the H_2 electronic transitions is produced by singlet systems in the 700 Å to1800 Å region of the spectrum, for the electron temperatures considered here. Seven band systems account for virtually all of the discrete emission; $C-X$, $D-X$, $B-X$, $B'-X$, $B''-X$, and $E, F-B$.

The ground state connected transitions are allowed with lifetimes of the order of 1 ns. The model calculations applied here include rotational fine structure transitions and take into account predissociation and self-absorption effects. The ground state connected Rydberg series transitions indicated above determine the populations of the upper states, because the radiative transition probabilities are much larger than the branches for other loss processes. The Rydberg transitions have typical electric dipole excitation functions. However, the cross-section for the direct excitation process,

$$e + H_2(X) \rightarrow H_2(E, F) + e,$$

shows a characteristic electron exchange dependence on electron energy (Ajello *et al.*

1983), because the symmetry of $E, F\ ^1\Sigma_g^+$ is the same as that of the ground state. The sharply rising cross-section for the excitation of the E, F state, near threshold (~12·5 eV), causes this state to dominate the production of extreme ultraviolet (EUV) radiation at the electron temperatures considered here, through the cascade process $E, F - B - X$. Unlike the other states in this model calculation, the E, F state is relatively long lived, with lifetimes ranging from 200 ns to 400 ns, as calculated by Glass-Maujean *et al.* (1983). Although it is assumed in the emission rate calculations that the E, F state is deactivated entirely by radiative transitions, the population in this case may be affected to some degree by collisional deactivation and excitation into the ionization continuum as discussed below. Emission rates for the electronic systems are given in Table 1 for two electron temperatures, $T_e = 1$, and 1·5 eV. The calculated spectrum for each of these cases is shown in figures 1 and 2, assuming that the observing instrument in this case was a spectrometer with 5 Å resolution. The major uncertainty in this calculation lies with the E, F state and possible collisional transfer to the $C\ ^1\Pi_u$ state under these excitation conditions. If this process turns out to be competitive with the $E, F - B$ radiative transition, the predicted spectra would be somewhat different from those shown in figures 1 and 2, but the radiative energy efficiency would remain essentially the same as stated in Table 1. An additional process affecting the E, F state may be electron excitation upward into the ionization continuum, contributing to the production of H_2^+ in the plasma. This reaction could therefore be of some importance in the plasma dynamics of the thyratron if the rate coefficient were competitive with the ionization of atomic hydrogen at some point in the discharge. Table 2 shows the coefficients calculated here. In this case the H_2 E, F state ionization collision strength has been calculated using the known generalized oscillator strength—Gaunt factor product at 300 eV (gf(300 eV) = 1·14) for the $H_2(X)$ ionization process, along with the $H_2(X)$ Gaunt factor shape function.

The excitation of the H_2 triplet states above the repulsive $b\ ^3\Sigma_u^+$ gives rise to the well known H_2 continuum, mainly through direct and cascade excitation of the $a\ ^3\Sigma_g^+$ state with subsequent $a - b$ transition radiation. The continuum emission tends to be complex and pressure dependent because the c, a, e and d states contribute measurably to the production of the spectrum (see Shemansky & Smith, 1983). Direct transitions to the repulsive b state from the c, e and d states are forbidden by symmetry properties, and the continuum is produced following the discrete transitions $c(v>0) - a$, $e - a$, and $d - a$ which give rise to visible and near infrared emission. The major contributor to the continuum is excitation of the $c(v>0)$ state, which has a radiative lifetime of $(v>0) \approx$ 100 μ sec (Freis & Hiskes, 1970). In this case the chamber pressure is low enough for most of the deactivation to appear as continuum emission (Fowler & Holzberlein 1965; 1966). The cross-sections for the excitation of the triplet states are characteristic of electron exchange processes and therefore peak at low energies in the 14–16 eV region. Therefore there is a tendency to produce copious emission in low temperature plasmas. The continuum spectrum ranges from ~1250 Å into the infrared with a peak differential emission rate in the 1300 Å to 2000 Å region. The triplet state spectrum is not shown here, but rate coefficients from Shemansky & Smith (1983) are used to calculate the total emission rates shown in Table 1. At the plasma temperatures considered here, the $a - b$ continuum transition is the dominant photon source, although the emission is spread over a broad spectral range.

3. Atomic excitation and radiative processes

The production efficiency of excited atomic levels can be found using a general collisional-radiative model (Bates *et al.* 1962a; Bates *et al.* 1962b), with the assumption

T_e (eV)	$C-X$	$D-X$	$D'-X$	$B-X$	$B'-X$	$B''-X$	$B-X$ (cont.)	$E,F-B$	$e+H_2 \rightarrow H(2P)+H+e$	All triplet systems (cont.)
1	1·76 (3)	4·29 (1)	8·26	3·43 (3)	5·66 (1)	5·92	2·77 (2)	6·33 (4)	7·08 (1)	2·53 (5)
	3·08 (−3)	8·73 (−5)	1·77 (−5)	5·12 (−3)	1·07 (−4)	1·21 (−5)	3·48 (−4)	9·28 (−2)	1·15 (−4)	2·80 (−1)
1·5	2·44 (5)	1·44 (4)	3·52 (3)	4·63 (5)	1·73 (4)	2·53 (3)	5·34 (4)	4·35 (6)	2·43 (4)	1·33 (7)
	5·23 (−1)	2·93 (−2)	7·56 (−3)	6·79 (−1)	3·28 (−2)	5·18 (−3)	7·08 (−2)	6·38	3·97 (−2)	1·46 (1)
$\bar{\varepsilon}$ (eV)	10·94	12·74	13·42	9·16	11·83	12·79	8·00	9·16	10·20	7·50

TABLE 1. Emission rates of the H_2 Rydberg Systems. The upper numbers give the radiation intensities of the systems, I_{rad} in 10^{12} photons/cm^3 s, whereas the lower numbers give the rate of radiation energy emission of the system ε_{rad} in W/cm^3. $\bar{\varepsilon}$ denotes the average radiated energy per photon. Parenthesis (l) represent the multiplication factors 10^l.

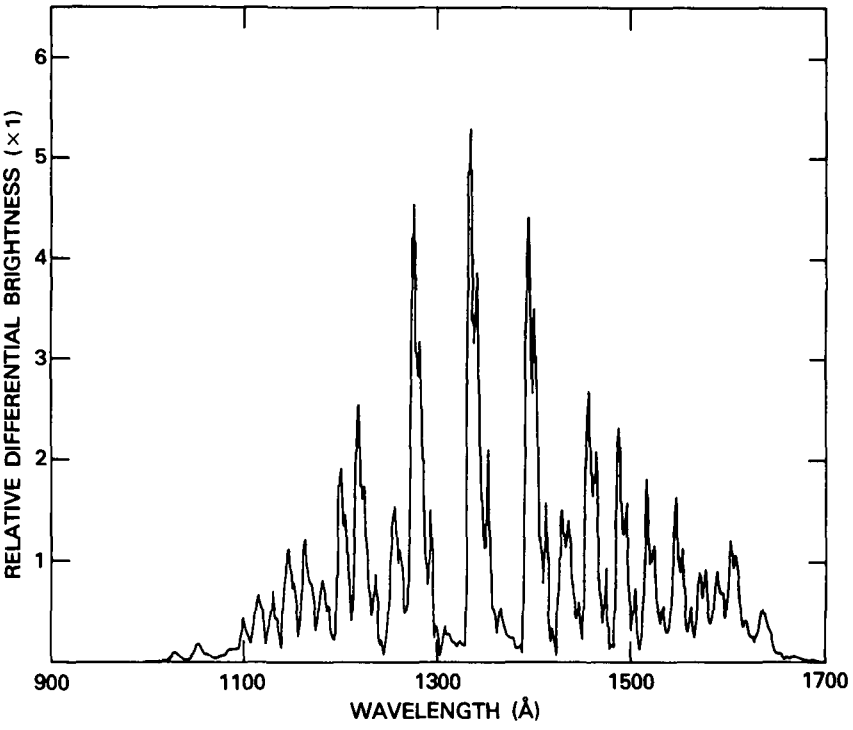

FIGURE 1. Spectrum of H_2 Rydberg states emission excited by electrons, $T_e = 1$ eV, observed through a 10^{16} cm^{-3} column of molecular hydrogen at a heavy particle temperature $T_h = 800$°K. Assumed resolution of the spectrum is 5·0 Å.

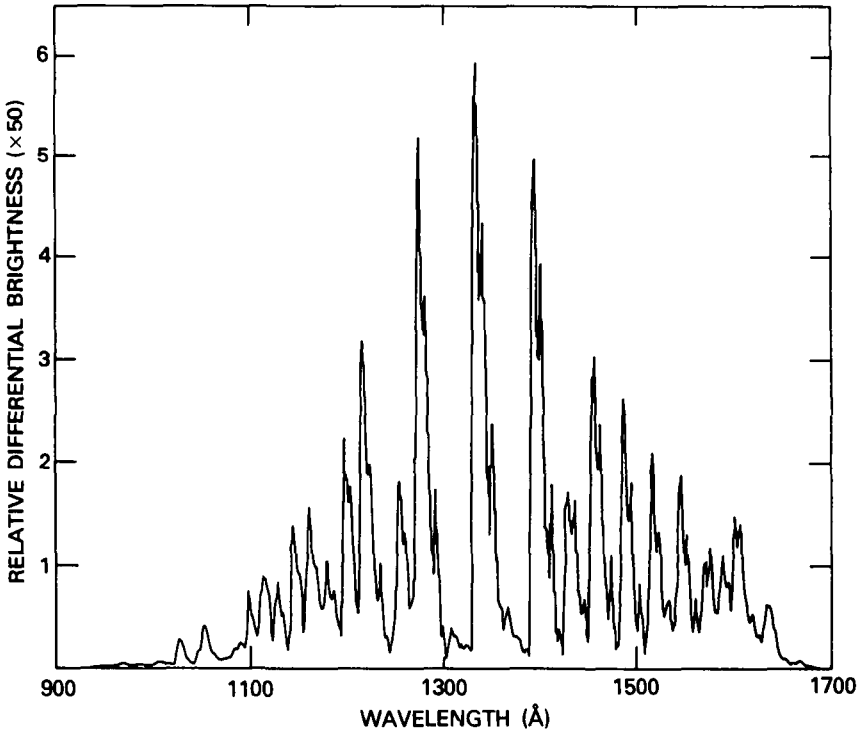

FIGURE 2. Spectrum of H_2 Rydberg states emission excited by electrons, $T_e = 1{\cdot}5$ eV, observed through a 10^{16} cm^{-3} column of molecular hydrogen at a heavy particle temperature $T_h = 800$°K. Assumed resolution of the spectrum is 5·0 Å.

T_e (eV)	ν_H^{ion} ($cm^{-3}s^{-1}$)	$\nu_{H_2(E,F)}^{ion}$ ($cm^{-3}s^{-1}$)
1	4·2 (19)	1·1 (16)
1·5	0·9 (21)	2·4 (18)

TABLE 2. The ionization rate coefficient frequencies ν^{ion} for electron impact ionization of some atomic and molecular hydrogen states. ν_H^{ion} is the rate coefficient for total ionization of atomic hydrogen. $\nu_{H_2(E,F)}^{ion}$ is the rate coefficient for ionization of E, F states of molecular hydrogen. Parenthesis (l) represent the multiplication factors 10^l.

that the major collisional process producing the excited atomic states is electron-atom collisions (Kunc *et al.* 1983). Radiation-induced transitions are negligible in this case (Hearn, 1963). The populations of excited atomic levels $N_{H(j)}$ are determined from a set of balance equations, one for each atomic level. Under the assumptions mentioned above this set of equations has the following form:

$$\frac{\partial N_{H(j)}}{\partial t} = \sum_{i<j} N_e N_{H(i)} S_{ij}^{I} + \sum_{i>j} N_e N_{H(i)} S_{ij}^{II} + \sum_{i>j} N_{H(i)} A_{ij} \kappa_{ij} + N_e N^+ (\alpha_j \kappa_{cj} + N_e \beta_j)$$
$$- N_{H(j)} \left(\sum_{i<j} N_e S_{ji}^{I} + \sum_{i<j} N_e S_{ji}^{II} + \sum_{i<j} A_{ji} \kappa_{ji} + N_e S_{jc} \right),$$
$$j = 1, 2, \ldots, j_{max}, \quad (1)$$

where $N_{H(j)}$ is the population of the atoms on the jth energy level, N_e and N^+ are electron and ion densities, respectively. S_{ij}^{I} and S_{ji}^{II} are rate coefficients for electron impact excitation from a lower level i to a higher level j and for electron impact de-excitation from the level j to level i, respectively, S_{cj} is the rate coefficient for electron impact ionization from level j. The factors α_j and β_j are rate coefficients for radiative recombination and for three-body recombination into level j, respectively. A_{ji} is the spontaneous transition probability and j_{max} is the maximum number of excited levels taken into consideration. The coefficients κ_{ji} and κ_{cj} (for radiative transitions between discrete states and for radiative recombination, respectively), called 'escape factors', take into account the effect of radiation trapping (Holstein 1951; Hearn 1963).

The radiation escape factors κ_{ji} were introduced as a convenient way to represent multiple reabsorption of radiation in the plasma. The term $N_j A_{ji} \kappa_{ji}$ in equations (1) represents the combined effects of spontaneous emission and radiative excitation, i.e., the sum,

$$N_j A_{ji} + N_i B_{ij} (\pi/c) \int_0^\infty \hat{I}(\nu) f(\nu)\, d\nu, \quad (2)$$

where $I(\nu)$ is the intensity of radiation averaged over direction and B_{ij} is the Einstein coefficient for the radiation absorption which can be easily expressed in terms of the spontaneous emission coefficient A_{ji}. Therefore, the escape factor can be given in the

following form,

$$\kappa_{ji} = 1 - \frac{N_i g_j c^2}{N_j g_i 2h(\nu_{ji}^0)^3} \int_0^\infty \hat{I}(\nu) f(\nu)\, d\nu, \tag{3}$$

where ν_{ji}^0 is the central frequency of the line.

Equation (3) couples the balance equations (1) with the radiative transfer equation. The problem of finding the escape factors is complicated. The method of McWhirter (1965) seems to be justified in this plasma and gives the escape factors as function of the mean optical depth τ_{ji} at the central frequency of the line ν_{ji}^0 i.e.,

$$\kappa_{ji}(\tau_{ji}) = 1 + \sum_k (-1)^k \frac{(\tau_{ji})^k}{(k+1)^{\frac{1}{2}} k!}, \tag{4}$$

where the mean optical depth τ_{ji} for the line produced in the $j \rightarrow i$ transition is given by Bates *et al.* (1962b).

The radiative recombination spectrum of H^+ shows a strong continuum feature beginning at 911 Å and continuing to shorter wavelengths, corresponding to recombination into the H (1 s) state. The total recombination coefficient and the spectral shape of the continuum emission has a distinct dependence on temperature. The total recombination cross-section is known and is calculated from the photoionizaton cross-section given by the Milne relation (Osterbrock, 1974). The recombination rates are given in Table 3, along with the emission rates for the two temperatures considered here. The spectrum of the continuum is shown in Figure 3, normalized to indicate the spectral change with temperature. It was assumed here that the major ion in the plasma is H^+ (Kunc *et al.* 1983; Kunc & Gundersen 1983a). The calculations of the continuum emission spectrum are based on the Brown & Matthews (1970) formulation.

4. Radiation power loss efficiency

The estimated energy efficiency for the production of the H_2 Rydberg system and H Lyman and Balmer series emissions can be calculated by using the results presented in Tables 1 and 3. This efficiency is defined for the steady-state phase of the discharge considered here as the following,

$$\lambda = \lambda_{H_2} + \lambda_H, \tag{5}$$

with,

$$\lambda_{H_2} = \frac{(\varepsilon_{\text{rad}}^{\text{tot}})_{H_2}}{\vec{j} \cdot \vec{E}} \quad \text{and} \quad \lambda_H = \frac{(\varepsilon_{\text{rad}}^{\text{tot}})_H}{\vec{j} \cdot \vec{E}}, \tag{6}$$

where $(\varepsilon_{\text{rad}}^{\text{tot}})_{H_2}$ and $(\varepsilon_{\text{rad}}^{\text{tot}})_H$ are total energy emission rates for all transitions (specified in Tables 1 and 3) of molecular and atomic hydrogen, respectively. $\vec{j}$ is the the electron current density and $\vec{E}$ is the electric field of the steady-state discharge. The last two quantities are equal to about 60 A/cm^2 and 10 V/cm, respectively in a characteristic steady-state discharge of the high-current thyratron. All quantities in relationships (5) and (6) are presented in Table 4.

5. Discussion

One of the more important uncertainties in the calculation of radiative properties of the discharge relates directly to the fundamental question of what processes contribute to the ionization of the gas during the conduction phase. The estimation of the ionization rate quantities depends critically on an accurate estimate of the electron

T_e (eV)	L_α	L_β	L_γ	L_δ	H_α	H_β	H_γ	$H^+ \rightarrow H$ (1 s) (cont.)
1	3·50 (3)	2·15 (2)	1·30 (2)	1·07 (2)	7·96 (4)	6·31 (3)	2·14 (3)	1·62 (3)
	5·71 (−3)	4·16 (−4)	2·72 (−4)	2·08 (−4)	2·42 (−2)	2·58 (−3)	9·77 (−4)	3·52 (−3)
1·5	1·17 (5)	3·14 (4)	2·61 (4)	2·43 (4)	8·52 (6)	1·31 (6)	4·82 (5)	1·20 (3)
	1·91 (−1)	6·57 (−2)	5·29 (−2)	4·97 (−2)	2·58	5·35 (−1)	2·19 (−1)	2·64 (−3)
$\bar{\varepsilon}$ (eV)	10·2	12·09	12·75	13·05	1·89	2·55	2·85	14·56 (T_e = 1 eV) 15·01 (T_e = 1·5 eV)

TABLE 3. Emission rates of the H Lyman (L) and Balmer (H) lines. The upper numbers give the radiation intensities of the lines, I_{rad} in 10^{12} photons/cm^3, whereas the lower numbers give the rate of radiation energy emission of the line ε_{rad} in W/cm^3. $\bar{\varepsilon}$ denotes the average radiated energy per photon. Parenthesis (l) represent the multiplication factors 10^l.

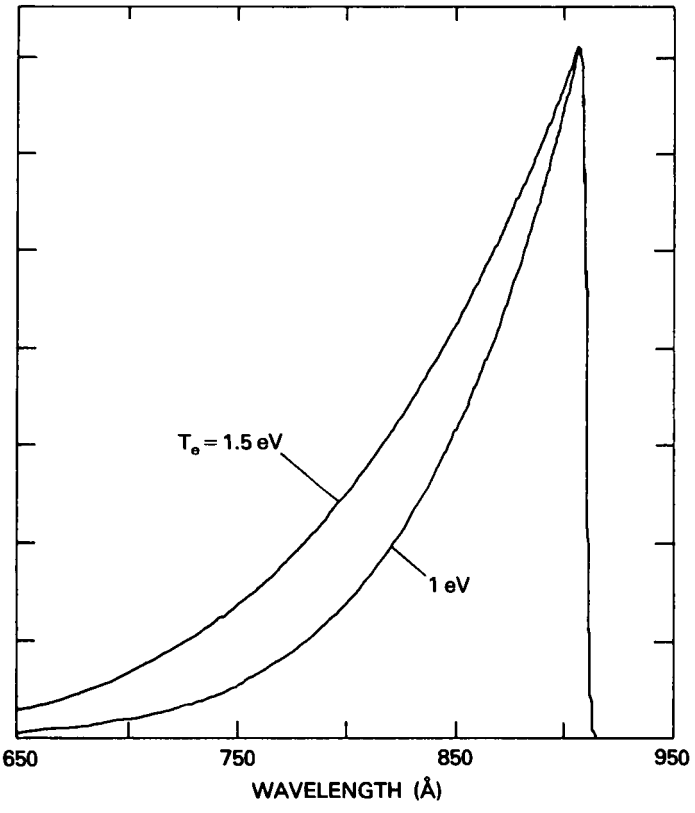

FIGURE 3. Differential brightness of the H_2 radiative recombination continuum as a function of wavelength in the EUV, calculated at electron temperatures $T_e = 1{\cdot}0$ and $1{\cdot}5$ eV. The spectrum is shown as modeled for observation using a spectrometer with an assumed 5 Å FWHM resolution. The recombination curves are normalized at the peak value to illustrate the temperature dependence of the continuum distribution. The absolute intensity scales for the two curves are in the ratio 1:0·553.

energy distribution. Observation of the radiative characteristics can probably provide the best measure of the electron distribution, but in addition more accurate estimates of ionization cross-sections for excited states such as the $H_2(E, F)$ levels are required. The rates for ionization of $H_2(E, F)$ levels are given in Table 2. Another factor affecting ionization rates is the entrapment of radiation in the atomic hydrogen system because this process has a tendency to change the population of the excited states. Ions can be produced from excited atomic states by subsequent collisions with electrons or absorption of non-resonant photons. The calculation of the state of atomic hydrogen in the

T_e (eV)	$(\varepsilon^{tot}_{rad})_{H_2}$ (W/cm^3)	$(\varepsilon^{tot}_{rad})_H$ (W/cm^3)	λ_{H_2}	λ_H	λ
1	2·90 (−1)	3·79 (−2)	4·83 (−4)	6·32 (−5)	5·46 (−4)
1·5	2·22 (1)	3·69	3·70 (−2)	6·15 (−3)	4·31 (−2)

TABLE 4. The estimated power efficiencies for production of H_2 and H emission in the nominal volume (1 cm^3) in the steady-state discharge. The steady-state electron current density $j = 60$ A/cm^2 and the electric field $|\vec{E}| = 10$ V/cm. Parenthesis (l) represent the multiplication factors 10^l.

present case is difficult, as noted above, and the calculations contain some uncertainties which are outlined below.

The approach leading to the escape factors given through equations (3) and (4) has been criticized (Biaz & Pham 1972; Kogan 1967; and Suckewer & Kuszell 1975) as being valid only in the center of the volume and being less appropriate as an approximation in the vicinity of the gas boundary. However, generalizations of the escape factors have been proposed (Hearn 1966; Suckewer & Kuszell 1975). These generalizations take into account an anisotropy of radiation, and match the boundary conditions consistently. The approach of Suckewer and Kuszell (1975) proposes the generalization of Holstein factors for multilevel atoms using a non-coupling approximation. However, the accuracy of such an approximation for multilevel atoms is still open to question, and requires a separate analysis.

It should be added that plasmas under conditions close to those considered here are optically thin for all molecular lines except for transitions into the H_2 ($X\Sigma_g^+, v=0$) level. The efficiency of conversion of the H_2 optically thick lines into optically thin radiation in the EUV tends to be high, so that the radiative energy in this process is delivered immediately to the chamber walls. The gas is also optically thin for all atomic lines except the Lyman series. The transmission of the Lyman series lines in the gas is a strong function of principal quantum number (n). In this case the gas is optically thin to lines originating from $n>14$ levels. The levels $14>n>2$ are optically thick to varying degrees and the radiative energy is lost mostly through conversion to the optically thin Balmer series transitions. The Lyα (1216 Å) transition is a special case because the upper state has no other radiative branch for the loss of energy. Thus, neglecting other factors, all of the optically thick Lyα radiation may be delivered to the walls of the chamber. In reality some uncertain fraction of the Lyα radiation will be lost to absorption by trace impurities in the gas, excitation into the ionization continuum by electrons and photons and to H_2 fluorescence through frequency redistribution caused by the multiple scattering process. The production of ionization from excited atomic levels becomes an important factor because of the fact that the majority electron mean energy in the discharge tends to be low. The determination of the H ($n>1$) populations in the optically thick gas therefore tends to be important for an understanding of the dynamics of the discharge. The estimated ionization rates and rate coefficients (Erwin & Kunc 1983) for atomic hydrogen in the nominal thyratron are included in Table 2. The rate quantities in Table 2 are given for the total H system. The electronic excited states for H are the dominant sources of ionization in the optically thick gas. The substantial contribution to the production of ions from excited states in H emphasizes the important effect radiation entrapment may have on the discharge and is one means by which trace impurities in the gas may affect discharge conditions and conduction phase lifetimes. The observation of the EUV emission characteristics of the discharge is therefore an important factor in understanding the process, because this region of the spectrum is most sensitive to the physical parameters.

The magnitude of the escape factor for the Lyα line applied in the present calculations is $\kappa_{21} \approx 10^{-3}$. As discussed above, this quantity at present has some degree of uncertainty. The long time scales of the multiple scattering process relative to the discharge pulse time raises the point that treating the discharge as a steady state condition is only an approximation.

6. Conclusion

From Table 1 it is seen that the most energetically intense H_2 Rydberg system radiation is continuum radiation of all triplet states. In the case of atomic radiation

(Table 3) the most energetically intense radiation is the optically thin Balmer alpha (H_α) line and potentially the Lyα line. All of the energy in the H_2 Rydberg systems is lost by EUV radiation. The strong radiative recombination radiation is only weakly affected by absorption processes.

Another important conclusion is that both molecular and atomic radiation emissions are strongly dependent on electron temperature T_e in the range considered here, i.e. from $T_e = 1$ eV to $T_e = 1{\cdot}5$ eV. The power efficiencies λ_H, λ_{H_2} and λ (Table 4) show a similar tendency, in that they increase with elecron temperature, reaching about five percent at $T_e = 1{\cdot}5$ eV. The radiative power emitted by atomic and molecular transitions is only a very small fraction of total power of a high-current thyratron plasma under typical steady-state conditions. However, the characteristics of the emitted radiation, especially in the EUV region are sensitive to the details of the physical processes controlling the discharge and obviously hold the key to understanding the complexities of the thyratron.

It is clear that the observation of EUV emission in the hydrogen thyratron is vital to the understanding of the breakdown and conductive process. Thre relative intensities of the H^+ radiative recombination and H_2 emission are very sensitive to the electron temperature and should provide precise temperature measurements. The spectrum of the H_2 discrete band systems is sensitive to deviation from a Maxwellian in the energy distribution of the electrons. The H^+ recombination continuum also provides an independent measure of electron temperature. The absolute value of the H^+ recombination coefficient is accuratedly known and deviations in rates from expected values could be taken as a measure of the presence of other ions such as H_3^+, an important question for the dynamics of the plasma.

Acknowledgements

This work was supported by the Air Force Office of Scientific Research, the Army Research Office and the Department of Energy.

REFERENCES

AJELLO, J. M., SHEMANSKY, D. E., KWOK, L. & YOUNG, Y. L. 1984 *Phys. Rev.* **A29,** 636.

BATES, D. R., KINGSTON, A. E. & MCWHIRTER. 1962a *Proc. Roy. Soc.* **A267,** 297.

BATES, D. R., KINGSTON, A. E. & MCWHIRTER. 1962b *Proc. Roy. Soc.* **A270,** 155.

BIAZ, T. & PHAM, D. W. 1972 *J. Phys. B,* **5,** 198.

BROWN, R. L. & MATTHERS, W. G. 1970 *Astroph. J.* **160,** 939.

CAIRNS, R. B. & SAMPSON, J. A. R. 1966 *J. Opt. Soc. Am.* **56,** 1568.

ERWIN, D. A. & KUNC, J. A. 1983 *IEEE Trans. Plasma Science,* **11,** 266.

FOWLER, R. G. & HOLZBERLEIN, T. M. 1965 *J. Chem. Phys.* **42,** 3723.

FOWLER, R. G. & HOLZBERLEIN, T. M. 1966 *J. Chem. Phys.* **45,** 1123.

FREIS, R. P. & HISKES, J. R. 1970 *Phys. Rev. A,* **2,** 573.

GLASS-MAUJEAN, M., DESSLER, K. & QUADRELLI, L. 1983 *Physics. Rev.* **A28,** 2868.

HEARN, A. G. 1963 *Proc. Phys. Soc.* **81,** 648.

HEARN, A. G. 1966 *Proc. Phys. Soc.* **88,** 171.

HISKES, J. R. 1982 *Proc. of 35th Inter. Gas. Electr. Conf., Dallas.*

HISKES, J. R., KARA, A. M., BACAL, M., BRUNETAU, A. M. & GRAHAM, W. G. 1982 *J. Appl. Phys.* **53,** 3469.

HOLSTEIN, T. 1951 *Phys. Rev.* **83,** 1159.

KOGAN, V. I. 1967 *Proc. of 8th Inter. Conf. on Phenomenon in Ionized Gases, Vienna.*

KUNC, J. A. & GUNDERSEN, M. A. 1982 *IEEE Trans. on Plasma Sci., Special Issue,* **10,** 315.
KUNC, J. A., GUHA, S. & GUNDERSEN, M. A. 1983 *Laser and Particle Beams,* **1,** 395.
KUNC, J. A. & GUNDERSEN, M. A. 1983a *Laser and Particle Beams,* **1,** 407.
KUNC, J. A. & GUNDERSEN, M. A. 1983b *J. Appl. Phys.* **54,** 2761.
MCWHIRTER, R. W. P., *Plasma Diagnostic Techniques, Academic Press,* 1965.
OSTERBROCK, D. E., *Astrophysics of Gaseous Nebulae, Freeman and Co.,* 1974.
SHEMANSKY, D. E. & AJELLO, J. M. 1983 *J. Geophys. Res.* **88,** 459.
SHEMANSKY, D. E. & SMITH, G. R. 1984 *submitted.*
SUCKEWER, S. & KUSZELL, A. 1975 *J. Quant. Spectr. Rad. Transfer,* **16,** 53.